

Article

## Evaluating Spectral Indices for Assessing Fire Severity in Chaparral Ecosystems (Southern California) Using MODIS/ASTER (MASTER) Airborne Simulator Data

Sarah Harris <sup>1,2</sup>, Sander Veraverbeke <sup>2,\*</sup> and Simon Hook <sup>2</sup>

<sup>1</sup> School of Geography and Environmental Science, Monash University, Melbourne, VIC 3800, Australia; E-Mail: sarah.harris@monash.edu

<sup>2</sup> Jet Propulsion Laboratory, California Institute of Technology, 4800 Oak Grove Drive, Pasadena, CA 91109, USA; E-Mail: Simon.J.Hook@jpl.nasa.gov

\* Author to whom correspondence should be addressed; E-Mail: Sander.S.Veraverbeke@jpl.nasa.gov; Tel.: +1-818-354-0278; Fax: +1-818-354-5148.

Received: 20 September 2011; in revised form: 18 October 2011 / Accepted: 18 October 2011 /

Published: 11 November 2011

---

**Abstract:** Wildland fires are a yearly recurring phenomenon in many terrestrial ecosystems. Accurate fire severity estimates are of paramount importance for modeling fire-induced trace gas emissions and rehabilitating post-fire landscapes. We used high spatial and high spectral resolution MODIS/ASTER (MASTER) airborne simulator data acquired over four 2007 southern California burns to evaluate the effectiveness of 19 different spectral indices, including the widely used Normalized Burn Ratio (NBR), for assessing fire severity in southern California chaparral. Ordinal logistic regression was used to assess the goodness-of-fit between the spectral index values and ordinal field data of severity. The NBR and three indices in which the NBR is enhanced with surface temperature or emissivity data revealed the best performance. Our findings support the operational use of the NBR in chaparral ecosystems by Burned Area Emergency Rehabilitation (BAER) projects, and demonstrate the potential of combining optical and thermal data for assessing fire severity. Additional testing in more burns, other ecoregions and different vegetation types is required to fully understand how (thermally enhanced) spectral indices relate to fire severity.

**Keywords:** fire severity; burn severity; Normalized Burn Ratio; emissivity; surface temperature; southern California; chaparral; MASTER

---

## 1. Introduction

Fire regimes are characterized by their spatial pattern, frequency, intensity, seasonality, size distribution and severity [1]. In recent years, measurements of severity have gained importance. Severity is a valuable substitute for fire intensity when data on fire intensity are unavailable. Fire intensity describes the physical combustion process in terms of energy release from organic matter [2]. As a result, fire intensity is generally expressed in energy fluxes. Severity, in contrast, is more general in gauging the fire impact. This impact can be described as: (i) the amount of damage [3-5]; (ii) the physical, chemical and biological changes [6-10]; or (iii) the degree of alteration [11,12] that fire causes to an ecosystem. In this context, the terms fire severity and burn severity are often used interchangeably [2], however, Lentile *et al.* [13] and Veraverbeke *et al.* [14], suggest a clear distinction between both terms by considering the fire disturbance continuum [15], which addresses three different temporal fire effects phases: before, during and after the fire. In this framework fire severity quantifies the short-term fire effects in the immediate post-fire environment while burn severity quantifies both the short- and long-term impact as it includes response processes. A precise assessment of fire/burn severity is essential to: (i) obtain more reliable estimates of burning efficiency, which is a crucial parameter for evaluating greenhouse gas emissions [16]; and to (ii) contribute to a better understanding of fire regimes, regenerative strategies of species, successional pathways and hydro-geomorphological effects. These important objectives strengthen the need for a better understanding of fire/burn severity as an integral component in ecosystem functioning.

From a mono- and bi-temporal point of view conceptually simple band ratioing as well as more sophisticated approaches, such as spectral unmixing and radiative transfer models (RTMs), have been used to estimate wildfire severity, traditionally with moderate resolution Landsat imagery. RTMs consider the whole spectral profile and are physically based [17-20]. The main advantage of these simulation models is that their performance is site-independent which greatly enhances their applicability and inter-comparability over a wide range of ecosystems [18,20]. Spectral mixture analysis (SMA) applied to post-fire images have resulted in fractional ground cover measures closely related to burning efficiency, usually implementing at least the green vegetation and charred soil endmembers [21-23]. SMA proved to be efficient in detecting the charcoal signal even in lightly burned areas that kept a strong vegetation signal. Unmixing is therefore advantageous because of its ability to distinguish between burns and other sparsely vegetated areas [24]. The most popular approach, however, can be found in ratioing band reflectance data. In this context, the Normalized Burn Ratio (NBR) has become accepted as the standard spectral index to assess the severity of fire [25-29]. The NBR relates to vegetation moisture content by combining near infrared (NIR) with short wave infrared (SWIR) reflectance. Pre-and post-fire ratio images are often bi-temporally differenced, resulting in the differenced layers, which permit a clear distinction between burned and unburned region [27]. The bi-temporal index approach, however, can be constrained by limitations in image availability [28], which reduces the chances for acquiring the ideal anniversary date image couple [29,30]. For this reason, extracting critical post-fire information from a single scene can be of particular interest.

Previous research has demonstrated that the performance of the NBR approach varies among ecoregions and vegetation types [26,27,31-33]. Consequently, there is need to independently validate the approach for specific regions and vegetation types [13,26,34,35] to determine if the technique is

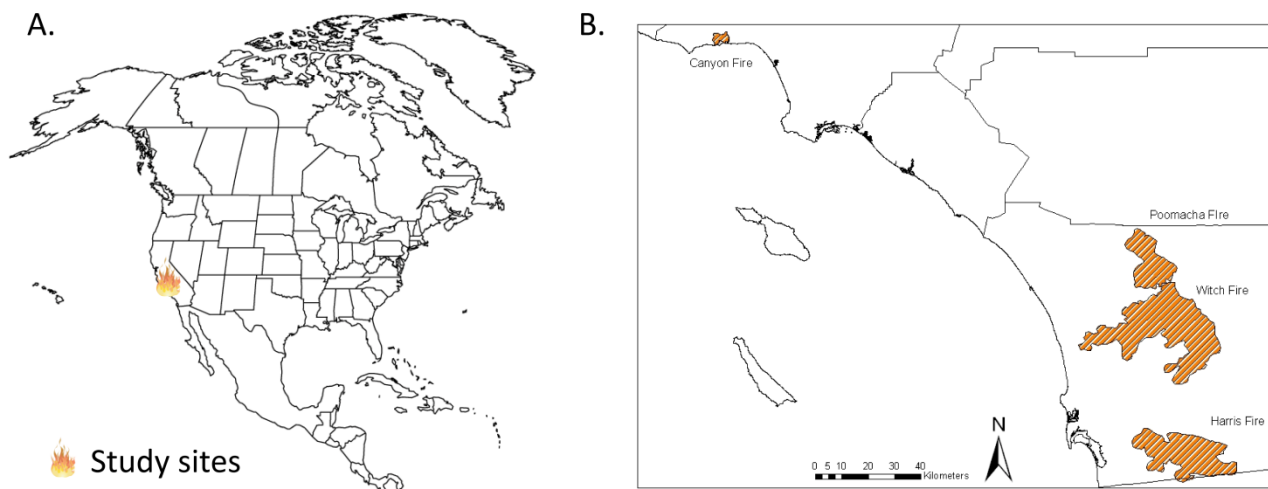
capable of inferring fire/burn severity from satellite imagery [31]. The Landsat NBR is used as a post-fire management tool in the USA and Canada, e.g., as operationally used by the Burned Area Emergency Rehabilitation (BAER) teams in the conterminous USA [12]. Numerous studies have demonstrated the usefulness of the index in the North American boreal and temperate regions [11,31,36-38], however, far fewer studies have assessed its effectiveness in California chaparral shrublands [9,20,39], an ecosystem which is highly sensitive to burning [39-41]. The few studies in the California chaparral shrublands demonstrated that the NBR is reasonably well related to fire severity, however, none of them conducted an inter-indices comparison. In Mediterranean shrublands in Europe similar findings were obtained by De Santis and Chuvieco [18], Veraverbeke *et al.* [32,33], Escuin *et al.* [42] and Tanase *et al.* [43]. Limited comparisons with other spectral indices were undertaken by De Santis and Chuvieco [18], Veraverbeke *et al.* [32,33] and Escuin *et al.* [42] concluding that the NBR outperformed the Normalized Difference Vegetation Index (NDVI) for assessing fire severity in Mediterranean shrublands. In addition, several authors indicated that the post-fire temperature increase as observed in the thermal infrared (TIR) domain [44,45] is complementary to the NBR for discriminating burned areas [46-48]. Holden *et al.* [46] demonstrated that enhancing the NBR with Landsat's thermal band resulted in a better separability between burned and unburned land for two wildland fires in New Mexico, USA, whereas Veraverbeke *et al.* [48] revealed the potential of combining optical and thermal imagery for discriminating burned areas. In the study of Veraverbeke *et al.* [48] the prospect of enhancing the NBR with thermally derived surface emissivity was shown for separating burned areas in southern California. This study aims to evaluate the performance of existing vegetation indices and thermally enhanced indices for assessing fire severity in chaparral ecosystems. The study uses MODIS/ASTER (MASTER) airborne simulator data acquired over four southern California fire scars. MASTER was developed to support scientific studies by the Advanced Spaceborne Thermal Emission Radiometer (ASTER) and MODerate resolution Imaging Spectroradiometer (MODIS) projects [49]. These high spatial and high spectral resolution data provide a unique opportunity for an in-depth evaluation of the sensitivities of several indices to fire severity in chaparral ecosystems.

## 2. Methodology

### 2.1. Study Area

Wildfires are a yearly recurring phenomena in southern California [20,41,50]. In the 2007 fire season 23 separately named fires burned over 200,000 ha. These fires mainly occurred in mountainous terrain and were driven by the strong Santa Ana winds, which are known to create extreme fire conditions in the region [51]. Four of the 2007 southern California wildfires were selected for this study. These fires are called the Canyon fire, the Harris fire, the Poomacha fire and the Witch fire (Figure 1). The fires occurred in October 2007 during a Santa Ana event. The main vegetation type consumed during these fires was chaparral. Chaparral is a complex and distinctive shrub formation that dominates the hills and lower mountain slopes of California. In southern California chaparral occupies approximately 70% of the land below the pine forests [50]. Composed of evergreen, woody shrubs, it often forms extensive and almost impenetrable stands. It is strongly adapted to protracted yearly drought and it is prone to recurrent fires, but vigorous in its recovery [20].

**Figure 1.** Location of the study sites in southern California.



2.2. Field Data

Assessments of fire severity were obtained using the field protocol described in the Fire Monitoring Handbook (FMH, [52]). 25 field plots were established in November 2007, within one month after the fires. The plots were selected taking into account the constraints on mainly accessibility and time, encompassing the range of variability in fire severity in the study areas. To minimize potential misregistration the plots were GPS-recorded in relatively homogeneous areas in terms of post-fire effects. The FMH protocol is based on a visual rating assessment. Both fire effects on substrate and vegetation were separately judged. A description of the five fire severity classes for both substrate and vegetation is given in Table 1. Ratings range between five (high fire severity) and one (unburned). Figure 2 shows the distribution of the field plots over the different severity classes.

**Figure 2.** Distribution of the field plots over the fire severity (FS) classes.

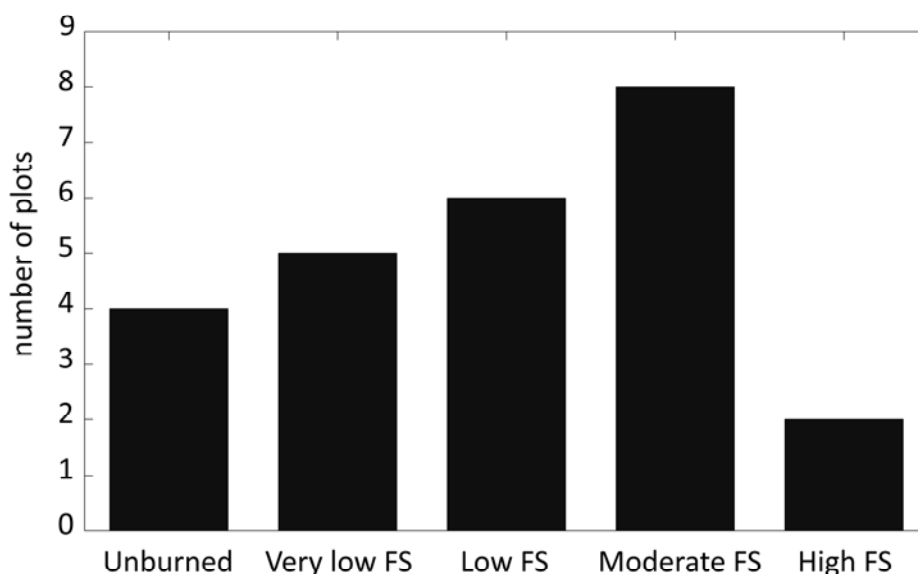


**Table 1.** Description of the fire severity classes for both substrate and vegetation (after [41]).

Fire severity Class	Substrate	Vegetation
Unburned (1)	Not burned	Not burned
Very low (2)	Litter partially blackened; duff nearly unchanged; wood/leaf structures unchanged	Foliage scorched and attached to supporting twigs
Low (3)	Litter charred to partially consumed, some leaf structure undamaged; surface is predominantly black; some gray ash may be present immediately postburn; charring may extend slightly into soil surface where litter is sparse, otherwise soil is not altered	Foliage and smaller twigs partially to completely consumed; branches mostly intact; less than 60% of the shrub canopy is commonly consumed
Moderate (4)	Leaf litter consumed, leaving coarse, light colored ash; duff deeply charred, but underlying mineral soil is not visibly altered; woody debris is mostly consumed; logs are deeply charred, burned-out stump holes are common	Foliage, twigs, and small stems consumed; some branches (>0.6–1 cm in diameter) still present; 40–80% of the shrub canopy is commonly consumed
High (5)	Leaf litter completely consumed, leaving a fluffy fine white ash; all organic material is consumed in mineral soil to a depth of 1–2.5 cm, this is underlain by a zone of black organic material; colloidal structure of the surface mineral soil may be altered	All plant parts consumed leaving only stubs greater than 1 cm in diameter

### 2.3. MASTER Imagery and Preprocessing

The MASTER airborne simulator acquired high spectral and high spatial resolution imagery over the burned area in November 2007. The spatial resolution of MASTER data ranges from 5 m to 50 m depending on flying height. The pixel size of the data in this study varied between 6 and 8.5 m depending on the site. The instrument acquires radiance spectra between 0.4  $\mu\text{m}$  and 13  $\mu\text{m}$  in 50 spectral channels with 11 visible NIR (VNIR) channels, 14 SWIR channels and 25 mid infrared (MIR) and TIR channels.

The MASTER data were provided as level 1b geolocated calibrated radiance. Atmospheric and Topographic Correction for Airborne Imagery (ATCOR4) software was used to correct for the influence of the atmosphere, solar illumination and sensor viewing geometry [53]. ATCOR4 uses a large database containing the results of radiative transfer calculations based on MODTRAN4 code [53]. The standard ATCOR4 desert aerosol model was chosen. The visible through SWIR bands (1–25) were processed to surface reflectance, the MIR bands (26–40) were not atmospherically corrected and the thermal bands (41–50) were atmospherically corrected to surface radiance. The surface radiance of the thermal bands was then separated into surface temperature ( $T_s$ ) and surface emissivity ( $\epsilon$ ) using the emissivity normalization method [54].  $\epsilon$  is defined as the ratio of the actual emitted radiance to the radiance emitted from a blackbody at the same thermodynamic temperature [55,56]. Finally, the images were georeferenced using input geometry.

### 2.4. Spectral Indices

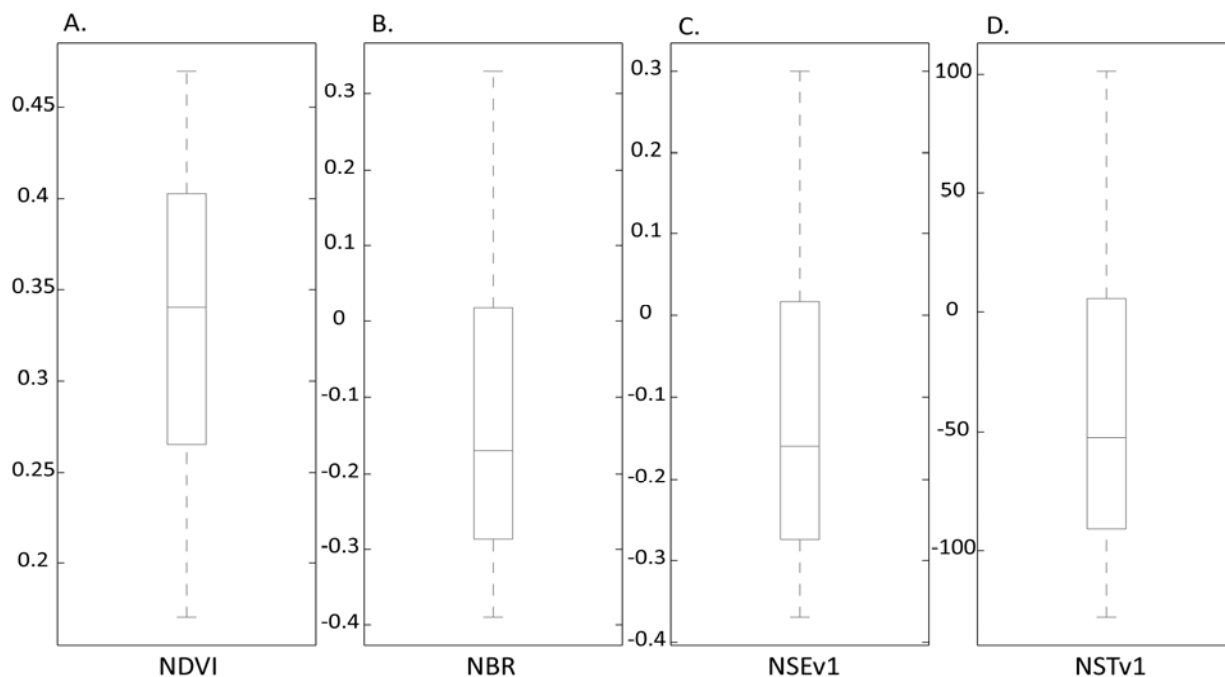
This study evaluates the performance of 19 spectral indices as listed in Table 2. This table includes: (i) the widely used NDVI [57], Global Environment Monitoring Index (GEMI, [58]) Enhanced

Vegetation Index (EVI, [59]), Soil Adjusted Vegetation Index (SAVI, [60]) and Modified Soil Adjusted Vegetation Index (MSAVI, [61]); (ii) indices specifically designed for burned land applications such as the Burned Area Index (BAI, [62]), GEMI3 [63], NBR [27], Char Soil Index (CSI, [64]) and Mid InfraRed Burn Index (MIRBI, [65]); and (iii) thermally enhanced spectral indices. The NDVI [57] is the most widely used index in ecological remote sensing because of its strong relation with above-ground biomass [66]. Several modifications of the NDVI have been proposed to minimize the influence of disturbing signals (mainly background and atmospheric effects). The GEMI aims to reduce atmosphere effects by proposing a non-linear index [58], whereas Huete *et al.* [59] achieved the same goal by taking advantage of the blue channel's sensitivity to atmosphere influences. In an attempt to reduce the influence of the background signal, Huete *et al.* [60] presented the SAVI which incorporates a soil-adjustment factor  $L$  in its formula (Table 2). SAVI is only an exact solution for bare soil if the soil line (the linear relationship between red and NIR reflectance of bare soils) slope and intercept equal respectively one and zero [61]. To overcome this limitation, Qi *et al.* [61] introduced the MSAVI by replacing SAVI's adjustment factor  $L$  by a self-adaptable correction factor that changes with changing vegetation density. By doing so, MSAVI theoretically further reduces background noise and enhances vegetation sensitivity. Kaufman and Remer [67] replaced the red band, which is traditionally used in VIs because of its high chlorophyll absorption property, by the mid infrared (MIR) spectral region relying on the fact that the latter spectral domain is related to vegetation moisture content, however, compared to the red band, the MIR region remains largely unaffected by aerosols. Only one index specifically designed for post-fire effects applications focuses on the red-NIR feature space, *i.e.*, the BAI [62]. The BAI aims to emphasize the charcoal signal in post-fire imagery by computing the bi-spectral distance from a pixel to a reference spectral point in the red-NIR space to which recently burned areas tend to converge [62]. Other burned land specific indices favor the SWIR and MIR regions because post-fire changes in these regions have shown to be more profound than those in the red region [32,42,46,47]. The NBR [27] is the resulting equivalent of the NDVI, whereas the GEMI3 [63] mimics the GEMI. In addition, the CSI is defined as the simple ratio between the NIR and SWIR reflectance [61], whereas the MIRBI only applies SWIR wavelengths [65]. Exploratory work of Holden *et al.* [46] and Smith *et al.* [47] and Veraverbeke *et al.* [48] demonstrated that enhancing existing indices with thermal imagery improved the separability of burned areas, in particular when these data was used as a complement to the NBR. These thermally enhanced indices are also listed in Table 2. The MASTER wavebands used in the indices of Table 2 were selected according to findings of Veraverbeke *et al.* [42] who analyzed the sensitivity to burned land of each spectral region ((blue (0.45–0.5  $\mu\text{m}$ ), red (0.6–0.7  $\mu\text{m}$ ), NIR (0.7–1.3  $\mu\text{m}$ ), shorter SWIR (sSWIR, 1.3–1.9  $\mu\text{m}$ ), longer SWIR (lSWIR, 1.9–2.5  $\mu\text{m}$ ), MIR (3–5.5  $\mu\text{m}$ ) and thermal infrared (TIR, 8–13  $\mu\text{m}$ )). The corresponding wavebands were 0.45–0.5  $\mu\text{m}$  (blue), 0.65–0.68  $\mu\text{m}$  (red), 0.86–0.88  $\mu\text{m}$  (NIR), 1.59–1.62  $\mu\text{m}$  (sSWIR), 2.31–2.36  $\mu\text{m}$  (lSWIR), 3.54–3.64  $\mu\text{m}$  (MIR) and 8.51–8.76  $\mu\text{m}$  (TIR) [45]. Figure 3 presents the box plots of the spectral index values from the field plots for the NDVI, NBR, NSEv1 and NSTv1.

**Table 2.** Spectral indices evaluated in this study (NIR: Near Infrared, sSWIR: shorter short wave infrared, lSWIR: longer short wave infrared, MIR: mid infrared, TIR: thermal infrared,  $\epsilon$ : emissivity and  $T_s$ : surface temperature, see Section 2.4 for specifications on wavelength intervals).

Index	Abbreviation and Reference	Formula
Normalized Difference Vegetation Index	NDVI [57]	$NDVI = \frac{NIR - red}{NIR + red}$
Global Environment Monitoring Index	GEMI [58]	$GEMI = \gamma(1 - 0.25\gamma) - \frac{red - 0.125}{1 - red}$ with $\gamma = \frac{2(NIR^2 - red^2) + 1.5NIR + 0.5red}{NIR + red + 0.5}$
Enhanced Vegetation Index	EVI [59]	$EVI = 2.5 \frac{NIR - red}{NIR - 6red - 7.5B + 1}$
Vegetation Index 3	VI3 [67]	$VI3 = \frac{NIR - MIR}{NIR + MIR}$
Soil Adjusted Vegetation Index	SAVI [60]	$SAVI = (1 + L) \frac{NIR - red}{NIR + red + L}$ with $L = 0.5$
Modified Soil Adjusted Vegetation Index	MSAVI [61]	$MSAVI = \frac{2NIR + 1 - \sqrt{(2NIR + 1)^2 - 8(NIR - red)}}{2}$
Burned Area Index	BAI [62]	$BAI = \frac{1}{(0.1 + red)^2 + (0.06 + NIR)^2}$
Global Environment Monitoring Index 3	GEMI3 [63]	$GEMI3 = \gamma(1 - 0.25\gamma) - \frac{MIR - 0.125}{1 - MIR}$ with $\gamma = \frac{2(NIR^2 - MIR^2) + 1.5NIR + 0.5MIR}{NIR + MIR + 0.5}$
Normalized Burn Ratio	NBR [27]	$NBR = \frac{NIR - lSWIR}{NIR + lSWIR}$
Char Soil Index	CSI [64]	$CSI = \frac{NIR}{SWIR}$
Mid InfraRed Burn Index	MIRBI [65]	$MIRBI = 10lSWIR - 9.8sSWIR + 2$
Normalized Difference Vegetation Index Thermal	NDVIT [47]	$NDVIT = \frac{NIR - red \times TIR}{NIR + red \times TIR}$
Soil Adjusted Vegetation Index Thermal	SAVIT [47]	$SAVIT = (1 + L) \frac{NIR - red \times TIR}{NIR + red \times TIR + L}$ with $L = 0.5$
Normalized Burn Ratio Thermal	NBRT [46]	$NBRT = \frac{NIR - lSWIR \times TIR}{NIR + lSWIR \times TIR}$
Vegetation Index 6 Thermal	VI6T [46]	$VI6T = \frac{NIR - TIR}{NIR + TIR}$
NIR-SWIR-Emissivity Version 1	NSEv1 [48]	$NSEv1 = \frac{NIR - lSWIR}{NIR + lSWIR} \times \epsilon$
NIR-SWIR-Emissivity Version 2	NSEv2 [48]	$NSEv2 = \frac{NIR - (lSWIR + \epsilon)}{NIR + lSWIR + \epsilon}$
NIR-SWIR-Temperature Version 1	NSTv1 [48]	$NSTv1 = \frac{NIR - lSWIR}{NIR + lSWIR} \times T_s$
NIR-SWIR-Temperature Version 2	NSTv2 [48]	$NSTv2 = \frac{NIR - (lSWIR + T_s)}{NIR + lSWIR + T_s}$

**Figure 3.** Box plots of the spectral index values from the field plots for the Normalized Difference Vegetation Index (NDVI, **(A)**), Normalized Burn Ratio (NBR, **(B)**), NIR-SWIR-Emissivity Version 1 (NSEv1, **(C)**) and NIR-SWIR-Temperature Version 1 (NSTv1, **(D)**).



### 2.5. Logistic Regression Analysis

Considering the ordinal nature of the field data, ordinal logistic regression analysis was performed [68]. Logistic regression has demonstrated to be a powerful method to assess the performance of spectral indices with nominal or ordinal response data [69-71]. The ordinal regression in this study used the fire severity field classes as dependent variable and the spectral index values as independent variables. The ordinal logistic regression model for a single independent variable is [68]:

$$\ln \left[ \frac{\pi_i(x)}{1-\pi_i(x)} \right] = \alpha_i + \beta_i x \quad (1)$$

where  $\pi_i(x)$  represents the probability of occurrence of the ordinal class  $i$  given the independent variable  $x$ . Separate intercept  $\alpha_i$  and slope  $\beta_i$  coefficients are calculated for each ordinal class  $i$ . A logistic model uses the maximum likelihood approach to estimate regression coefficients. The goodness-of-fit of the ordinal logistic regression model can be estimated by the deviance  $D$ , which is defined as [68]:

$$D = -2 \sum_i^m \sum_j^n \left[ y_{i,j} \times \ln \left( \frac{\hat{\pi}_{i,j}}{y_{i,j}} \right) + (1 - y_{i,j}) \times \ln \left( \frac{1 - \hat{\pi}_{i,j}}{1 - y_{i,j}} \right) \right] \quad (2)$$

where  $y_{i,j}$  denotes a dichotomous outcome variable for class  $i$  and  $\hat{\pi}_{i,j}$  is the maximum likelihood estimate of  $\pi_i(x_j)$ ,  $m$  is the number of ordinal classes and  $n$  is the sample size. Deviance can be thought of in a similar way as the residual sum of squares in ordinary linear regression models. A lower  $D$  values thus represent a better goodness-of-fit. In this study  $D$  was used to compare the performance of the different spectral indices as predictor variables for the fire severity field classes.

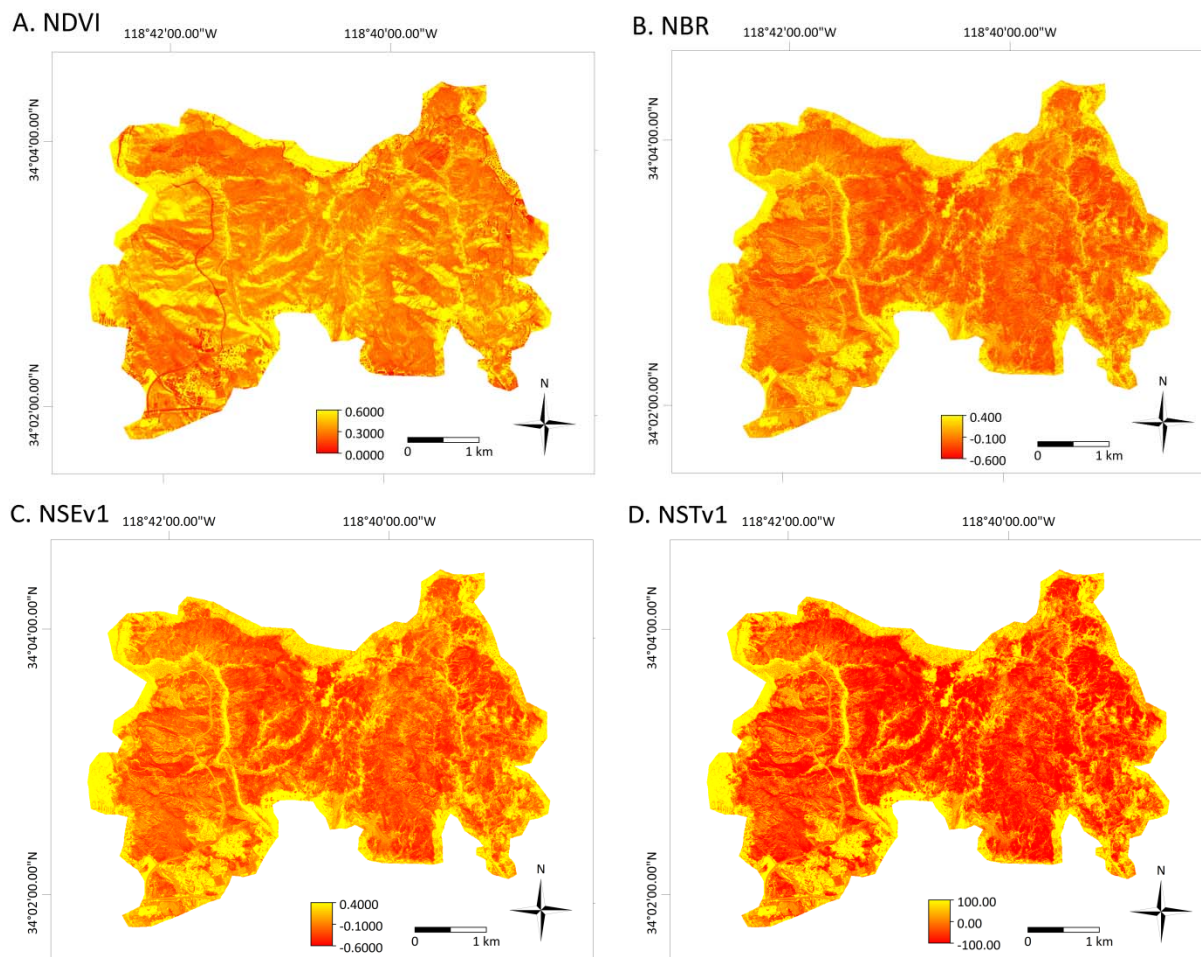
### 3. Results and Discussion

The best goodness-of-fit of the ordinal logistic regression model was obtained for the NSTv1 index which had a  $D$  of 64.24. Similar performance was observed with the NBR ( $D = 64.34$ ), NSEv1 ( $D = 64.50$ ) and NSEv2 ( $D = 64.55$ ). Moderate goodness-of-fit values ( $D$  between 65 and 72) were achieved by the CSI ( $D = 66.77$ ), NBRT (67.81), SAVI (70.26), VI3 (70.68) and NDVI (71.15). Weaker logistic regression models were achieved by the NDVIT, NSTv2, SAVIT, GEMI, GEMI3, VI6T, BAI, EVI, MIRBI and MSAVI ( $D > 72$ ). Table 3 lists the spectral indices according to the goodness-of-fit measure  $D$ . Figure 4 shows the NDVI, NBR, NSEv1 and NSTv1 spectral index maps of the Canyon fire.

**Table 3.** Spectral indices listed according to the deviance obtained from the ordinal logistic regression.

Spectral Index	Deviance ( $D$ )
NSTv1	64.24
NBR	64.34
NSEv1	64.50
NSEv2	64.55
CSI	66.77
NBRT	67.81
SAVI	70.26
VI3	70.68
NDVI	71.15
NDVIT	72.27
NSTv2	73.59
SAVIT	73.91
GEMI	73.94
GEMI3	74.36
VI6T	74.53
BAI	74.76
EVI	74.83
MIRBI	76.19
MSAVI	76.19

**Figure 4.** Spectral index maps for the Normalized Difference Vegetation Index (NDVI, **(A)**), Normalized Burn Ratio (NBR, **(B)**), NIR-SWIR-Emissivity Version 1 (NSEv1, **(C)**) and NIR-SWIR-Temperature Version 1 (NSTv1, **(D)**) of the Canyon fire (October 2007).



This study represents the first documented work to evaluate the effectiveness of different spectral indices for assessing fire severity in chaparral shrublands of southern California. Although the study is of limited scale several conclusions can be drawn. Our results support the current use of NBR by the BAER teams who use the NBR as a conceptually simple data layer to rapidly infer critical post-fire information in a cost-effective manner. Knowledge of how well the index relates to fire severity in shrubland ecosystems is essential if the NBR is to be used as a land management tool in California chaparral ecosystems. Results confirm the reasonably good performance of the NBR in chaparral [20,39] and Mediterranean shrublands [18,32,33,42,43]. In studies in other ecosystems than shrublands assessing the correlation between several spectral indices and field data, Epting *et al.* [26] ranked the NBR as the first index in single date and bi-temporal approaches. Similar findings were obtained by Hoy *et al.* [72] reporting that dNBR outperforms the differenced NDVI (dNDVI). In our study, however,  $D$  is still relatively high, even for the indices with the best performance. Previous studies have demonstrated that the suboptimal performance can be explained by the fact that fire-induced reflectance changes are only seldom perpendicular to the index isolines [29,32]. This suggests that improved index design or alternative methods have the potential to improve remotely sensed fire

severity assessments. Previous studies also found that the correlation between the NBR or the differenced NBR (dNBR), has a tendency to be higher for forested ecosystems than for more sparsely vegetated vegetation types such as shrubs [26,33,73]. Epting *et al.* [26] found a strong correlation for forested classes. More sparsely vegetated classes (e.g., shrubs, herbs), however, underperformed. Veraverbeke *et al.* [33] also found that the correlations in forest land were clearly stronger than those in sparser vegetation types. Another explanation for the only moderate-high correlation found in this chaparral study could be the November timing of the image acquisition. In this period of the year chaparral shrubs generally have low moisture content which might affect the performance of the indices which include a SWIR or MIR band. Results showed, however, that indices with a SWIR or MIR spectral band still yielded better results than indices lacking a SWIR or MIR band. This corroborates earlier research findings. Pereira [74] reported that AVHRR (Advanced Very High Resolution Radiometer) spectral indices based on the NIR and MIR channels had a higher discriminatory potential for burned surface mapping than indices based on the NIR and R channels. Trigg and Flasse [65] demonstrated the importance of the MIR region for burned shrub-savannah discrimination with MODIS data.

In contrast to their beneficial performance for discriminating burned areas [46,47], the thermally enhanced versions of the NDVI, SAVI and NBR did not improve the fire severity assessment. The NIR-SWIR- $\epsilon$  (NSE) indices and the NIR-SWIR- $T_s$  version 1 (NSTv1), however, obtained correlations with field data of severity similar to the NBR. These indices were developed by Veraverbeke *et al.* [48] and demonstrated to improve burned area estimations in southern California. The relatively poor performance of the NSTv2 can be explained by its index design. Due to the differences in absolute values between  $T_s$  and reflectance data, the NSTv2 index is dominated by the  $T_s$  data. We are not aware of any other studies that have explored the potential of remotely sensed  $\epsilon$  information in fire severity applications and there are only a smaller number of studies have assessed the utility of temperature data. This study shows that thermal data could be complementary to existing NIR-SWIR indices for assessing fire severity, in particular the NBR, however, more rigorous testing in a large variety of ecosystems is needed. Such studies are particularly important as NASA continues to develop new sensors with multiple spectral bands in the thermal infrared such as the planned Hyperspectral Infrared (HyspIRI) HyspIRI sensor (<http://hyspiri.jpl.nasa.gov/>). Due to the characteristic temporal dynamics of the post-fire environment, the utility of adding  $T_s$  in the fire severity assessment will heavily depend on the post-fire acquisition timing [14,59,75]. Veraverbeke *et al.* [75] showed that, although the post-fire  $T_s$  is long lasting, the magnitude of change rapidly alters as time elapses after the fire. This is because seasonal variation in meteorological conditions highly influences  $T_s$  development. Therefore, the prospect of remotely sensed  $T_s$  as fire severity indicator appears to be limited to the first post-fire month. Taking into account Landsat's 16-day revisiting time and the necessity of acquiring a cloud-free image [28], the potential of the  $T_s$  layer is even more constrained, however, sensor such as HyspIRI which have a 5-day revisit will address this problem. In contrast, emissivity is an inherent property of the surface and relates to cover type and soil moisture [76]. As such gradual post-fire recovery changes and seasonal variations in emissivity are likely to be longer lasting than temperature changes and complement the NIR and SWIR reflectance layers for fire severity retrievals. We believe that the full potential of remotely sensed emissivity  $\epsilon$  as fire severity indicator has only begun to be explored by

this study and additional studies with larger datasets and in other ecoregions and vegetation types are encouraged.

As stated by Hook *et al.* [49] the main aim of MASTER is to support scientific studies of current and future satellite sensors (in particular ASTER and MODIS). The need for scheduling flight lines and the relatively high cost restrict MASTER's suitability for regional scale fire severity mapping. The sensor's superior spectral and spatial resolution, however, permits an improved understanding of ecological remote sensing. In the context of assessing fire severity, this study: (i) supports the use of the NBR as indicator for fire severity in southern California chaparral as in operational use by the BAER teams; (ii) confirmed the utility of a MIR spectral band; and (iii) demonstrated the potential of thermal component as a complement to the NBR. To retrieve  $\epsilon$  from TIR imagery, at least three separate TIR bands are required [58,77]. Currently, ASTER is the only moderate resolution sensor in orbit that offers the opportunity of  $\epsilon$  retrieval. Unfortunately, since May 2008, ASTER no longer acquires reliable SWIR data due to the degradation of the detector's cooler system which causes saturation problems. The planned HypsIRI sensor, however, will combine the optical and thermal spectral domains. This will potentially open new perspectives for the remote sensing of post-fire effects. Our findings can also be of interest for other future satellite missions, such as the Landat Data Continuity Mission (LDCM).

#### 4. Conclusions

This letter addressed the need for validating existing fire severity indices in specific ecosystems; in this case southern California chaparral shrublands. The study made use of the beneficial spatial and spectral resolution of the MODIS/ASTER airborne simulator. 19 different indices, including the traditionally used Normalized Burn Ratio (NBR), were compared using field data of severity. Results: (i) support the operational use of the NBR by the Burned Area Emergency Rehabilitation project in chaparral shrublands; and (ii) reveal the potential of thermally enhanced spectral indices in fire severity applications. Additional experiments in southern California and other ecosystems are needed to fully assess the potential of enhancing the NBR with temperature and emissivity data to assess fire severity.

#### Acknowledgments

The research described in this paper was carried out at the Jet Propulsion Laboratory (JPL), California Institute of Technology, under a contract with the National Aeronautics and Space Administration. The authors would like to thank Marti Witter and Tim Handley of the National Park Service of the Santa Monica Mountains National Recreation Area, and Lorri Peltz-Lewis of the Department of Interior, US Bureau of Reclamation for supplying field data. The JPL authors' copyright for this publication is held by the California Institute of Technology. The authors would like to thank the anonymous reviewers for their constructive remarks.

#### References

1. Morgan, P.; Hardy, C.; Swetnam, T.; Rollins, M.; Long, D. Mapping fire regimes across time and space: understanding coarse and fine scale fire patterns. *Int. J. Wildland Fire* **2001**, *10*, 329-343.

2. Keeley, J. Fire intensity, fire severity and burn severity: A brief review and suggested usage. *Int. J. Wildland Fire* **2009**, *18*, 116-126.
3. Hammill, K.; Bradstock, R. Remote sensing of fire severity in the Blue Mountains: Influence of vegetation type and inferring fire intensity. *Int. J. Wildland Fire* **2006**, *15*, 213-226.
4. Gonzalez-Alonso, F.; Merino-De-Miguel, S.; Roldan-Zamarron, A.; Garcia-Gigorro, S.; Cuevas, J. MERIS Full Resolution data for mapping level-of-damage caused by forest fires: The Valencia de Alcántara event in August 2003. *Int. J. Remote Sens.* **2007**, *28*, 789-809.
5. Chafer, C. A comparison of fire severity measures: An Australian example and implications for predicting major areas of soil erosion. *Catena* **2008**, *74*, 235-245.
6. Landmann, T. Characterizing sub-pixel Landsat ETM+ fire severity on experimental fire in the Kruger National Park, South Africa. *South Afr. J. Sci.* **2003**, *99*, 357-359.
7. Chafer, C.; Noonan, M.; Macnaught, E. The post-fire measurement of fire severity and intensity in the Christmas 2001 Sydney wildfires. *Int. J. Wildland Fire* **2004**, *13*, 227-240.
8. Cocke, A.; Fule, P.; Crouse, J. Comparison of burn severity assessments using Differenced Normalized Burn Ratio and ground data. *Int. J. Wildland Fire* **2005**, *14*, 189-198.
9. Stow, D.; Petersen, A.; Rogan, J.; Franklin, J. Mapping burn severity of Mediterranean-type vegetation using satellite multispectral data. *GISci. Remote Sens.* **2007**, *44*, 1-23.
10. Lee, B.; Kim, S.; Chung, J.; Park, P. Estimation of fire severity by use of Landsat TM images and its relevance to vegetation and topography in the 2000 Samcheok forest fire. *J. Forest Res.* **2008**, *13*, 197-204.
11. Brewer, K.; Winne, C.; Redmond, R.; Opitz, D.; Mangrich, M. Classifying and mapping wildfire severity: A comparison of methods. *Photogramm. Eng. Remote Sensing* **2005**, *71*, 1311-1320.
12. Eidenshink, J.; Schwind, B.; Brewer, K.; Zhu, Z.; Quayle, B.; Howard, S. A project for monitoring trends in burn severity. *Fire Ecol.* **2007**, *3*, 3-21.
13. Lentile, L.; Holden, Z.; Smith, A.; Falkowski, M.; Hudak, A.; Morgan, P.; Lewis, S.; Gessler, P.; Benson, N. Remote sensing techniques to assess active fire characteristics and post-fire effects. *Int. J. Wildland Fire* **2006**, *15*, 319-345.
14. Veraverbeke, S.; Lhermitte, S.; Verstraeten, W.W.; Goossens, R. The temporal dimension of differenced Normalized Burn Ratio (dNBR) fire/burn severity studies: The case of the large 2007 Peloponnese wildfires in Greece. *Remote Sens. Environ.* **2010**, *114*, 2548-2563.
15. Jain, T.; Pilliod, D.; Graham, R. Tongue-tied. *Wildfire* **2004**, *4*, 22-26.
16. Andreae, M.; Crutzen, P. Atmospheric aerosols: Biogeochemical sources and role in atmospheric chemistry. *Science* **1997**, *276*, 1052-1058.
17. Chuvieco, E.; Riano, D.; Danson, F.; Martin, P. Use of a radiative transfer model to simulate the postfire spectral response to burn severity. *J. Geophys. Res.* **2006**, *111*, G04S09
18. De Santis, A.; Chuvieco, E. Severity estimation from remotely sensed data: Performance of simulation versus empirical models. *Remote Sens. Environ.* **2007**, *108*, 422-435.
19. De Santis, A.; Chuvieco, E.; Vaughan, P. Short-term assessment of burn severity using the inversion of PROSPECT and GeoSail models. *Remote Sens. Environ.* **2009**, *113*, 126-136.
20. De Santis, A.; Asner, G.; Vaughan, P.; Knapp, D. Mapping burn severity and burning efficiency in California using simulation models and Landsat imagery. *Remote Sens. Environ.* **2010**, *114*, 1535-1545.

21. Rogan, J.; Yool, S. Mapping fire-induced vegetation depletion in the Peloncillo mountains, Arizona and New Mexico. *Int. J. Remote Sens.* **2001**, *16*, 3101-3121.
22. Lewis, S.; Lentile, L.; Hudak, A.; Robichaud, P.; Morgan, P.; Bobbitt, M. Mapping ground cover using hyperspectral remote sensing after the 2003 Simi and Old wildfires in Southern California. *Fire Ecol.* **2007**, *3*, 109-128.
23. Robichaud, P.; Lewis, S.; Laes, D.; Hudak, A.; Kokaly, R.; Zamudio, J. Post-fire soil burn severity mapping with hyperspectral image unmixing. *Remote Sens. Environ.* **2007**, *108*, 467-480.
24. Rogan, J.; Franklin, J. Mapping wildfire burn severity in southern California forests and shrublands using Enhanced Thematic Mapper imagery. *Geocarto Int.* **2001**, *16*, 1-11.
25. Lopez-Garcia, M.; Caselles, V. Mapping burns and natural reforestation using Thematic Mapper data. *Geocarto Int.* **1991**, *6*, 31-37.
26. Epting, J.; Verbyla, D.; Sorbel, B. Evaluation of remotely sensed indices for assessing burn severity in interior Alaska using Landsat TM and ETM+. *Remote Sens. Environ.* **2005**, *96*, 328-339.
27. Key, C.; Benson, N. Landscape assessment: Ground measure of severity; The Composite Burn Index, and remote sensing of severity, the Normalized Burn Index. In *FIREMON: Fire Effects Monitoring and Inventory System*; Lutes, D., Keane, R., Caratti, J., Key, C., Benson, N., Sutherland, S., Gangi, L., Eds.; Rocky Mountains Research Station, USDA Forest Service: Fort Collins, CO, USA, 2005; pp. 1-51.
28. Ju, J.; Roy, D. The availability of cloud-free Landsat ETM+ data over the conterminous United States and globally. *Remote Sens. Environ.* **2008**, *112*, 1196-1211.
29. Veraverbeke, S.; Lhermitte, S.; Verstraeten, W.W.; Goossens, R. Illumination effects on the differenced Normalized Burn Ratio's optimality for assessing fire severity. *Int. J. Appl. Earth Obs. Geoinf.* **2010**, *12*, 60-70.
30. Verbyla, D.; Kasischke, E.; Hoy, E. Seasonal and topographic effects on estimating fire severity from Landsat TM/ETM+ data. *Int. J. Wildland Fire* **2008**, *17*, 527-534.
31. French, N.; Kasischke, E.; Hall, R.; Murphy, K.; Verbyla, D.; Hoy, E.; Allen, J. Using Landsat data to assess fire and burn severity in the North American boreal forest region: An overview and summary of results. *Int. J. Wildland Fire* **2008**, *17*, 443-462.
32. Veraverbeke, S.; Verstraeten, W.W.; Lhermitte, S.; Goossens, R. Evaluating Landsat Thematic Mapper spectral indices for estimating burn severity of the 2007 Peloponnese wildfires in Greece. *Int. J. Wildland Fire* **2010**, *19*, 558-569.
33. Veraverbeke, S.; Lhermitte, S.; Verstraeten, W.W.; Goossens, R. Evaluation of pre/post-fire differenced spectral indices for assessing burn severity in a Mediterranean environment with Landsat Thematic Mapper. *Int. J. Remote Sens.* **2011**, *32*, 3521-3537.
34. Cocks, A.; Fule, P.; Crouse, J. Comparison of burn severity assessments using Differenced Normalized Burn Ratio and ground data. *Int. J. Wildland Fire* **2005**, *14*, 189-198.
35. Fox, D.; Maselli, F.; Carrega, P. Using SPOT images and field sampling to map burn severity and vegetation factors affecting post forest fire erosion risk. *Catena* **2008**, *75*, 326-335.
36. Miller, J.; Yool, S. Mapping forest post-fire canopy consumption in several overstory types using multi-temporal Landsat TM and ETM data. *Remote Sens. Environ.* **2002**, *82*, 481-496.
37. van Wagendonk, J.; Root, R.; Key, C. Comparison of AVIRIS and Landsat ETM+ detection capabilities for burn severity. *Remote Sens. Environ.* **2004**, *92*, 397-408.

38. White, J.; Ryan, K.; Key, C.; Running, S. Remote sensing of forest fire severity and vegetation recovery. *Int. J. Wildland Fire* **1996**, *6*, 125-136.
39. Keeley, J.; Brennan, T.; Pfaff, A. Fire severity and ecosystem responses following fires in California shrublands. *Ecol. Appl.* **2008**, *18*, 1530-1546.
40. Peterson, S.; Moritz, M.; Morais, M.; Dennison, P.; Carlson, J. Modelling long-term fire regimes of southern California shrublands. *Int. J. Wildland Fire* **2011**, *20*, 1-16.
41. Westerling, A.; Bryant, B. Climate change and wildfire in California. *Climatic Change* **2008**, *87* Suppl. 1, S231-S249.
42. Escuin, S.; Navarro, R.; Fernandez, P. Fire severity assessment by using NBR (Normalized Burn Ratio) and NDVI (Normalized Difference Vegetation Index) derived from LANDSAT TM/ETM images. *Int. J. Remote Sens.* **2008**, *29*, 1053-1073.
43. Tanase, M.; Perez-Cabello, F.; de la Riva, J.; Santoro, M. TerraSAR-X data for burn severity evaluation in Mediterranean forest on sloped terrain. *IEEE Trans. Geosci. Remote Sens.* **2010**, *48*, 917-929.
44. Cahoon, D.; Stocks, B.; Levine, J.; Cofer, W.; Pierson, J. Satellite analysis of the severe 1987 forest fires in northern China and Southeastern Siberia. *J. Geophys. Res.* **1994**, *99*, 627-638.
45. Lambin, E.; Goyvaerts, K.; Petit, C. Remotely-sensed indicators of burning efficiency of savannah and forest fires. *Int. J. Remote Sens.* **2003**, *24*, 3105-3118.
46. Holden, Z.; Smith, A.; Morgan, P.; Rollins, M.; Gessler, P. Evaluation of novel thermally enhanced spectral indices for mapping fire perimeters and comparisons with fire atlas data. *Int. J. Remote Sens.* **2005**, *26*, 4801-4808.
47. Smith, A.; Drake, N.; Wooster, M.; Hudak, A.; Holden, Z.; Gibbons, C. Production of Landsat ETM+ reference imagery of burned areas within Southern African savannahs: Comparison of methods and application to MODIS. *Int. J. Remote Sens.* **2007**, *28*, 2753-2775.
48. Veraverbeke, S.; Harris, S.; Hook, S. Evaluating spectral indices for burned area discrimination using MODIS/ASTER (MASTER) airborne simulator data. *Remote Sens. Environ.* **2011**, *115*, 2702-2709.
49. Hook, S.; Myers, J.; Thome, K.; Fitzgerald, M.; Kahle, A. The MODIS/ASTER airborne simulator (MASTER)—A new instrument for earth science studies. *Remote Sens. Environ.* **2001**, *76*, 93-102.
50. Minnich, R. Fire mosaics in southern California and northern Baja California. *Science* **1983**, *213*, 1287-1294.
51. Keeley, J. Impact of antecedent climate on fire regimes in coastal California. *Int. J. Wildland Fire* **2004**, *13*, 173-182.
52. USDI National Park Service. *Fire Monitoring Handbook*; Fire Management Program Center, National Interagency Fire Center: Boise, ID, USA, 2003; pp. 1-274.
53. Richter, R. *Atmospheric/Topographic Correction for Airborne Imagery. ATCOR-4 User Guide*; Version 5.0; DLR-German Aerospace Center, Remote Sensing Data Center: Wessling, Germany, 2009; pp. 1-90.
54. Hook, S.; Gabell, A.; Green, A.; Kealy, P. A comparison of techniques for extracting emissivity information from thermal infrared data for geologic studies. *Remote Sens. Environ.* **1992**, *42*, 123-135.

55. Norman, J.; Becker, F. Terminology in thermal infrared remote-sensing of natural surfaces. *Agr. Forest Meteorol.* **1995**, *77*, 153-156.
56. Hulley, G.; Hook, S. The North American Land Surface Emissivity Database (NAALSED) Version 2.0. *Remote Sens. Environ.* **2009**, *113*, 1967-1975.
57. Tucker, C. Red and photographic infrared linear combinations for monitoring vegetation. *Remote Sens. Environ.* **1979**, *8*, 127-150.
58. Pinty, B.; Verstraete, M. GEMI—A nonlinear index to monitor global vegetation from satellites. *Vegetatio* **1992**, *101*, 15-20.
59. Huete, A.; Didan, K.; Miura, T.; Rodriguez, E.; Gao, X.; Ferreira, L. Overview of the radiometric and biophysical performance of the MODIS vegetation indices. *Remote Sens. Environ.* **2002**, *83*, 195-213.
60. Huete, A. A Soil-Adjusted Vegetation Index (SAVI). *Remote Sens. Environ.* **1988**, *25*, 295-309.
61. Qi, J.; Chehbouni, A.; Huete, A.; Kerr, Y.; Sorooshian, S. A modified soil adjusted vegetation index. *Remote Sens. Environ.* **1994**, *48*, 119-126.
62. Chuvieco, E.; Pilar Martin, M.; Palacios, A. Assessment of different spectral indices in the red-near-infrared spectral domain for burned land discrimination. *Remote Sens. Environ.* **2002**, *112*, 2381-2396.
63. Barbosa, P.; Gregoire, J.; Pereira, J. An algorithm for extracting burned areas from time series of AVHRR GAC data applied at a continental scale. *Remote Sens. Environ.* **1999**, *69*, 253-263.
64. Smith, A.; Wooster, M.; Drake, A.; Dipotso, F.; Falkowski, M.; Hudak, A. Testing the potential of multi-spectral remote sensing for retrospectively estimating fire severity in African savannahs. *Remote Sens. Environ.* **2005**, *97*, 92-115.
65. Trigg, S.; Flasse, S. An evaluation of different bi-spectral spaces for discriminating burned shrub-savanna. *Int. J. Remote Sens.* **2001**, *22*, 2641-2647.
66. Carlson, T.; Ripley, T. On the relation between NDVI, fractional vegetation cover and leaf area index. *Remote Sens. Environ.* **1997**, *62*, 241-252.
67. Kaufman, Y.; Remer, L. Detection of forests using Mid-IR reflectance: An application for aerosol studies. *IEEE Trans. Geosci. Remote Sens.* **1994**, *32*, 672-683.
68. Hosmer, D.; Lemeshow, S. *Applied Logistic Regression*; Wiley Series in Probability and Statistics; Wiley: New York, NY, USA, 2000; pp. 1-383.
69. Verbesselt, J.; Jonsson, P.; Lhermitte, S.; van Aardt, J.; Coppin, P. Evaluating satellite and climate data-derived indices as fire risk indicators in savanna ecosystems. *IEEE Trans. Geosci. Remote Sens.* **2006**, *44*, 1622-1632.
70. Lozano, J.; Suarez-Seoane, S.; de Luis, E. Assessment of several spectral indices derived from multi-temporal Landsat data for fire occurrence probability modelling. *Remote Sens. Environ.* **2007**, *107*, 533-544.
71. Malone, S.; Kobziar, L.; Staudhammer, C.; Abd-Elrahman, A. Modeling relationships among 217 fires using remote sensing of burn severity in southern pine forest. *Remote Sens.* **2011**, *3*, 2005-2028.
72. Hoy, E.; French, N.; Turetsky, M.; Trigg, S.; Kasischke, E. Evaluating the potential of Landsat TM/ETM+ imagery for assessing fire severity in Alaskan black spruce forest. *Int. J. Wildland Fire* **2008**, *17*, 500-514.

73. Allen, J.; Sorbel, B. Assessing the differenced Normalized Burn Ratio's ability to map burn severity in the boreal forest and tundra ecosystems of Alaska's national parks. *Int. J. Wildland Fire* **2008**, *17*, 463-475.
74. Pereira, J. A comparative evaluation of NOAA-AVHRR Vegetation Indexes for burned surface detection and mapping. *IEEE Trans. Geosci. Remote Sens.* **1999**, *37*, 217-226.
75. Veraverbeke, S.; Verstraeten, W.W.; Lhermitte, S.; Van De Kerchove, R.; Goossens, R. Spaceborne assessment of post-fire changes in vegetation, land surface temperature and surface albedo. *Int. J. Wildland Fire* **2011**, in press.
76. Hulley, G.; Hook, S.; Baldrige, A. Investigating the effects of soil moisture on thermal infrared land surface and emissivity using satellite retrievals and laboratory measurements. *Remote Sens. Environ.* **2010**, *114*, 1480-1493
77. Gillespie, A.; Rokugawa, S.; Matsunaga, T.; Cothorn, J.; Hook, S.; Kahle, A. A temperature and emissivity separation algorithm for Advanced Spaceborned Thermal Emission and Reflectance Radiometer (ASTER) images. *IEEE Trans. Geosci. Remote Sens.* **1998**, *36*, 1113-1126.

© 2011 by the authors; licensee MDPI, Basel, Switzerland. This article is an open access article distributed under the terms and conditions of the Creative Commons Attribution license (<http://creativecommons.org/licenses/by/3.0/>).